Role of MR and CT in Diagnostics

27

Josee Dubois and Gilles Soulez

MRI

MRI is the best method to evaluate the extension of the malformation and its relationship with adjacent structures [1]. The MR exam evaluates the extension; the size of the malformation; the infiltration of muscles, bones, tendons, and articulations; and the location of nerves, vessels, arteries, veins, and lymphatics included in the vascular malformations. MRI is also helpful in evaluating responses to treatment [2].

Routine sequences should include T1-weighted spin-echo or fast SE sequences, T2-weighted fat-suppressed fast SE acquisitions, and T1-weighted post-contrast fat-suppressed sequences. Depending on the clinical context and the result of Doppler US imaging, specific sequences are recommended depending whether we are investigating a slow- or fast-flow malformation.

Regarding slow-flow malformations, T1-weighted spin-echo sequences and T2-weighted fat suppression with short TI (inversion time) inversion recovery (STIR) are useful to determine the extent of the venous or lymphatic malformations. A T1-weighted spin-echo acquisition with fat suppression after gadolinium injection is required to document the enhancement of the malformation and differentiate venous malformation that will enhance from lymphatic malformation displaying minimal enhancement on the septa. 3D ultrafast spoiled gradient-echo acquisitions are also useful to evaluate the enhancement of the malformation after gadolinium injection. They can be repeated at different time frame to document the pattern of enhancement [3].

3D gadolinium-enhanced fat gradient-echo acquisition is helpful to evaluate the vascularization of the malformation [4]. To evaluate the dynamic circulation of the vascular anomalies, time-resolved MR angiography sequences are used and allow to differentiate the arterial inflow and venous drainage [5, 6].

CT Scan

Computed tomography plays a limited role for the evaluation of vascular anomalies given the inherent lack of soft tissue details and the advance of MR imaging. However, CT scan is useful for the evaluation of bone erosion and phleboliths, although last generation of multidetector CT can be used to obtain a three-dimensional reformation of vessels and to plan the embolization in cases of complex vascular anomalies. They are also useful to document aneurysm formation in high-flow malformations.

J. Dubois (✉)
Department of Medical Imaging,
CHU Sainte-Justine, Montreal, QC, Canada
e-mail: josee-dubois@ssss.gouv.qc.ca

G. Soulez
Department of Radiology,
CHUM Notre-Dame (University of Montreal),
Montreal, QC, Canada
e-mail: gilles.soulez.chum@ssss.gouv.qc.ca

R. Mattassi et al. (eds.), *Hemangiomas and Vascular Malformations: An Atlas of Diagnosis and Treatment*,
DOI 10.1007/978-88-470-5673-2_27, © Springer-Verlag Italia 2009, 2015

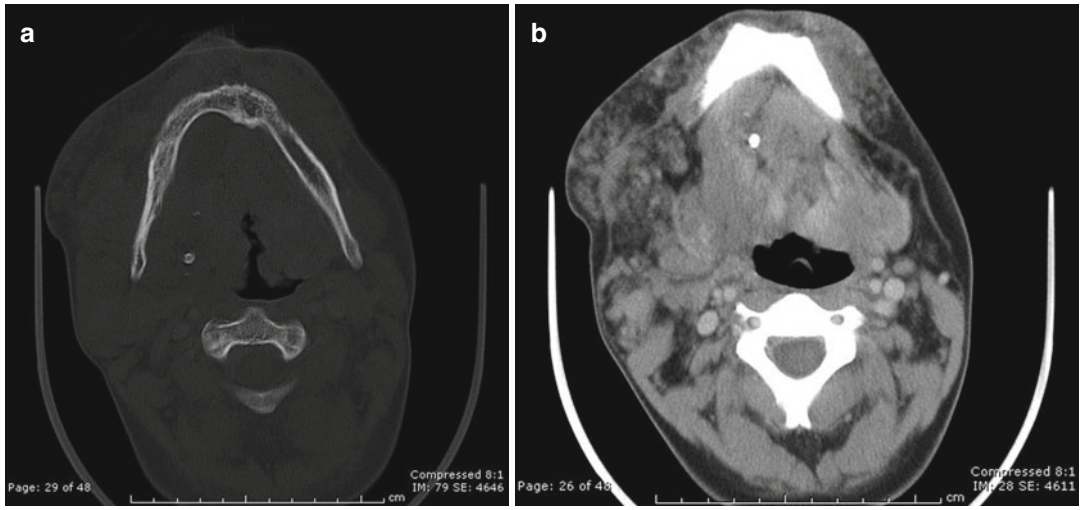

Fig. 27.1 Fourteen-year-old boy with venous malformation. (**a**, **b**) CT scan with contrast shows an extensive heterogeneous lesion of the face with infiltration of the masseter, buccal floor, tongue, parapharyngeal region, and mandibular bone. Phlebolith was seen

Venous Malformations

Different patterns of venous malformations (VMs) can be observed. The most common is a cavitary lesion with a delayed enhancement with or without abnormal draining vein. The second pattern is the presence of dysplastic veins that can be localized or diffuse in particular in upper or lower limbs. These patterns are better differentiated with percutaneous phlebography of the lesion before sclerotherapy.

Also, VMs can be a component of many syndromes, such as Klippel-Trénaunay, blue rubber bleb nevus, Maffucci's, Proteus, Cloves, or Bannayan-Riley-Ruvalcaba syndromes.

On *CT scan*, venous malformation shows a hypodense or heterogeneous lesion before contrast which enhances peripherally and slowly after injection of contrast. Phleboliths, bone erosion, or bony overgrowth is more clearly depicted on CT scan images (Fig. 27.1).

MRI – The first acquisition has to be done with a wide field of view to assess the extent of the lesion. VM can be seen on every part of the body. On T1-weighted images, VM is hypointense or isointense compared to the muscle. They may present with a heterogeneous or intermediate signal secondary to thrombosis or hemorrhage. Absence of flow void is mandatory for the diagnosis of VM. On fat-sat T2-weighted sequences, high-signal intensity is observed. Sometimes, low-signal intensity is related to thrombosis or phleboliths. Fat suppression with short TI (inversion time) inversion recovery (STIR) T2-weighted sequence with a 512 matrix is well suited for this purpose. T2-weighted gradient-echo sequences can also be used to demonstrate calcifications or hemosiderin. On gradient-echo sequences, the absence of signal in the blood vessel in the vicinity of the malformation suggests a slow-flow malformation. Fluid-fluid level can be seen in regions of low or no flow.

FSE T1-weighted sequences with fat suppression should be performed after gadolinium injection to evaluate the perfusion of the malformation. Heterogeneous enhancement is seen after injection of gadolinium. MRI may also demonstrate soft tissue changes related to the VM, such as fatty replacement, atrophy of the adjacent musculature, or hypertrophy of the subcutaneous fat compared with the contralateral side [7].

To evaluate the dynamics of the VM, we perform a dynamic perfusion study 1, 2, 5, and 10 min after contrast infusion using a 3D ultrafast spoiled gradient-echo acquisition (volumetric interpolated breath-hold examination (VIBE)

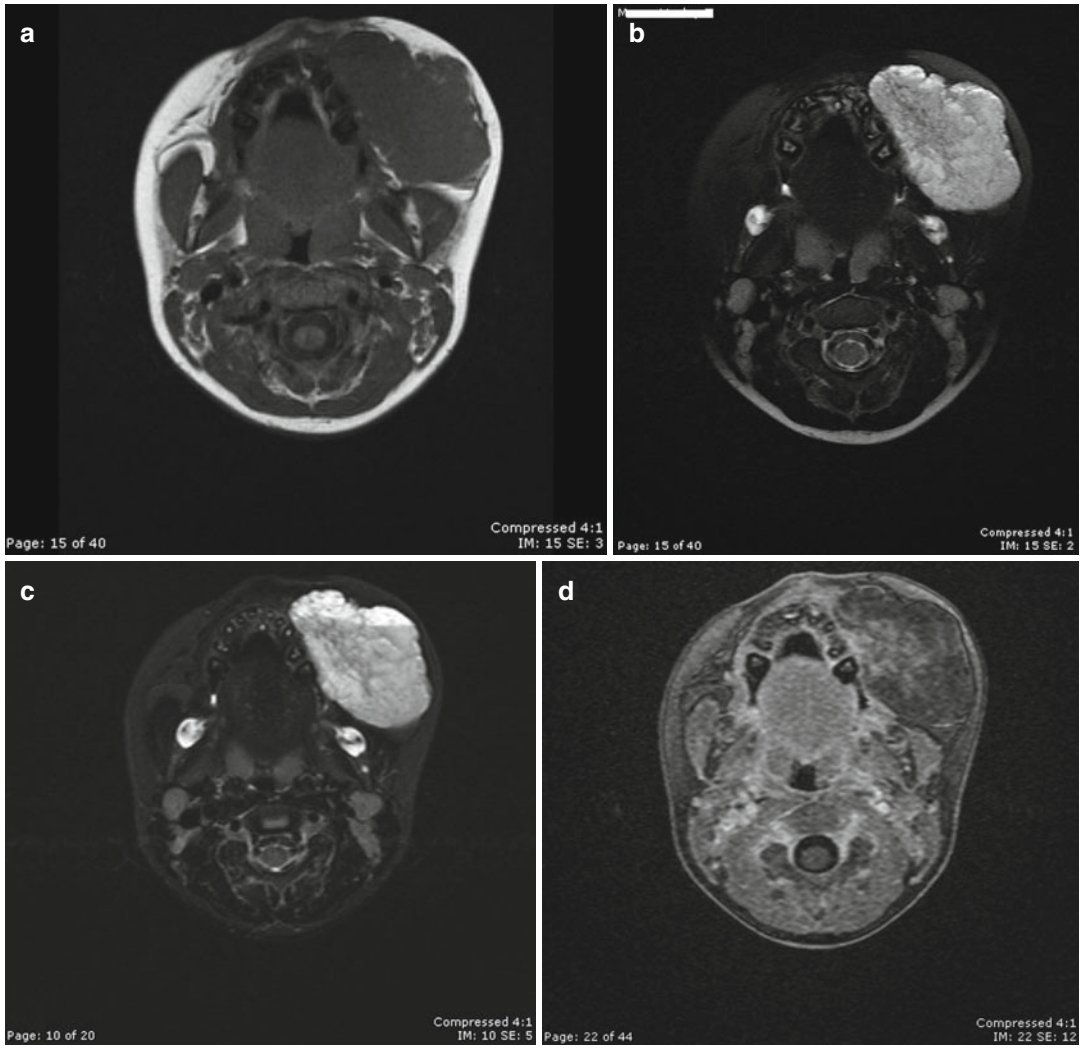

Fig. 27.2 Five-year-old girl with cheek venous malformation. (**a**) Axial T1-weighted image shows an isodense lesion of the left cheek. (**b**) Axial fast SE T2-weighted fat-suppressed image demonstrates a well-defined hyperintense lesion without perilesional edema. (**c**) STIR images show hyperintense lesion with small signal voids (phleboliths). (**d**) Dynamic VIBE acquisition was performed. At 10 min, heterogeneous filling of the malformation by gadolinium was seen

sequence). These contrast-enhanced 3D acquisitions are also useful to appreciate the drainage of the malformation in the venous system [1, 8].

On 3D contrast-enhanced MRA, the lesions and their drainage into the systemic venous system can be mapped and should be documented on the report. The absence of deep venous system can be a contraindication for sclerosing treatment in some complex cases (Figs. 27.2, 27.3, and 27.4).

Arteriovenous Malformations

Arteriovenous malformations (AVMs) are isolated anomalies or are part of a syndrome, such as Parkes Weber or Rendu-Osler-Weber.

On *CT scan*, AVMs appear as highly enhancing lesions with numerous feeding and draining vessels, without persistent tissue staining (Fig. 27.5).

MRI shows arteries and veins with low-signal intensity due to the flow void phenomenon

Fig. 27.3 Four-year-old girl with an extensive venous malformation of the hand. (**a**) Coronal axial T2 fat-suppressed image reveals a hyperintense signal of a significant infiltrative lesion of the muscle tendon of the hand. (**b**) STIR image shows the presence of hyperintense lesion with multiple phleboliths (*arrows*), seen as a signal void in the lesion. (**c**) Delayed contrast-enhanced fat-suppressed VIBE T1-weighted image shows diffuse enhancement of the venous malformation

of rapid and/or turbulent blood flow on both T1- and T2-weighted spin-echo sequences. Except for the presence of fat occasionally, no soft tissue mass is visible. A hypersignal is observed on gradient-echo and angiographic sequences. Occasionally, there are numerous interspersed small punctuated areas of high-signal intensity caused by hemorrhage and thrombosis. Gadolinium-enhanced MR angiography is helpful to evaluate feeding arteries and draining veins. The presence of an early venous filling is typically seen in AVMs. Using time-resolved MR angiography sequences, it is now possible to evaluate the dynamic opacification of AVM

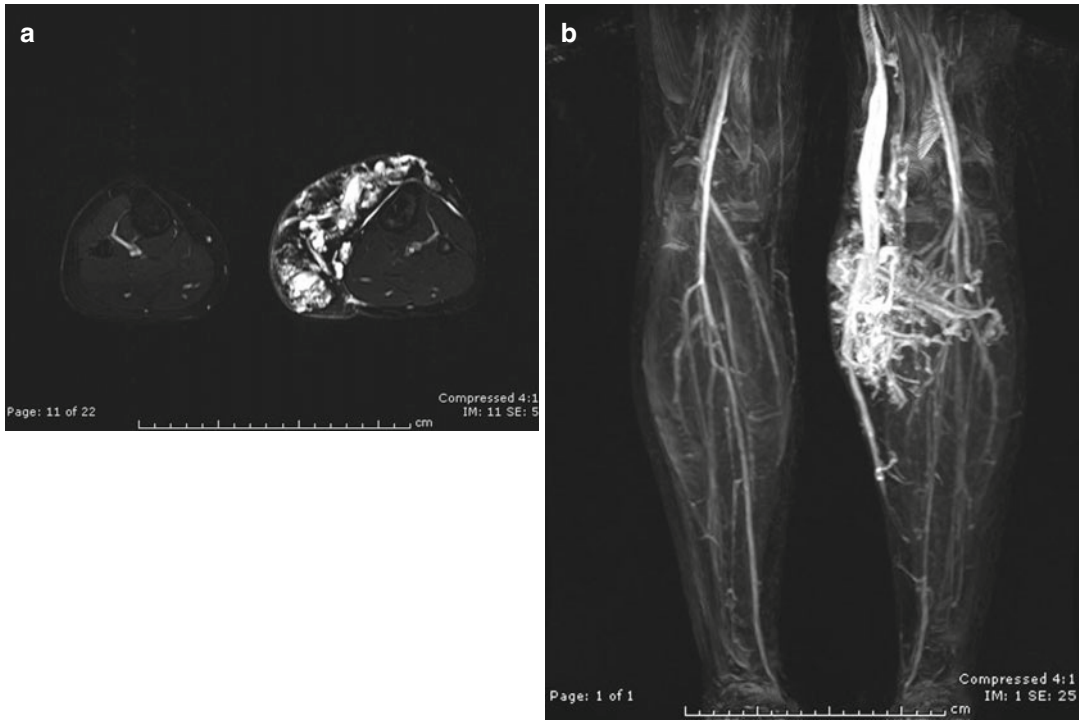

Fig. 27.4 Eighteen-year-old female with Klippel-Trénaunay syndrome. (**a**) Axial T2-weighted image demonstrates numerous hyperintense vessels in the subcutaneous fat. (**b**) Coronal contrast VIBE sub mip image shows numerous abnormal veins draining in a medial marginal vein. The deep venous system is normal

with the arterial feeders, nidus, and draining veins [6, 9, 10]. Since these sequences have a high temporal resolution, there is a compromise on spatial resolution which is lower than conventional 3D MR angiography using parallel imaging techniques (Fig. 27.6). In this setting, it can be useful to perform a 3D gradient-echo acquisition at high resolution during the steady-state phase of contrast enhancement to have a good delineation of the extension of the malformation.

Capillary Malformations

Capillary malformations are superficial vascular malformations. The only indication for MR imaging is to rule out an underlying AVM or associated complex anomalies such as Sturge-Weber, Klippel-Trénaunay, Parkes Weber, Cobb, or Proteus syndromes.

MRI – Capillary malformations are hyperintense on fluid-sensitive sequences and hypointense on T1-weighted images and display enhancement after contrast administration.

Lymphatic Malformations

Lymphatic malformations are divided into two types: macrocystic or microcystic. We will not discuss the lymphedema or complex syndrome associated with lymphatic malformations (Fig. 27.7).

CT scan of macrocystic lymphatic malformations shows a low-attenuation mass with enhancement of the septa after contrast injection [11].

Fig. 27.5 Patient presenting a pelvic AVM involving the right ovary and parameter. (**a**) Coronal reformation of a CTA in arterial phase showing the large AVM and the contribution of the right internal iliac artery (*large arrow*). Contributions of an enlarged right ovarian artery (*arrowhead*) and renal capsular arteries (*small arrow*) can be seen. (**b**) A large ovarian vein (*arrowhead*) draining the AVM is observed on a posterior coronal reformation. The proximal portion of the enlarged ovarian artery (*large arrow*) arising from an accessory renal artery (*small arrow*) is also demonstrated. (**c**) The extension and 3D anatomy of the AVM are well seen on this volume rendering reformation

A pure microcystic lymphangioma is ill defined with fat infiltration and no enhancement after contrast injection is observed.

MRI shows a septated mass with low-signal intensity on T1 and high-signal intensity on T2. Because of varying amounts of protein or hemorrhage within the lesion, lymphatic malformations occasionally present with variable-signal intensity on T1 and T2 sequences. Sometimes, a high signal on T1 sequence or a fluid level can be observed in cases of cyst with a high content of protein or a hemorrhagic content [3]. No gadolinium enhancement is visible, except in the septa. Pure microcystic lymphatic malformations are isointense on T1 and display a heterogeneous signal on T2, with or without a slight heterogeneous enhancement on T1 post gadolinium. Stranding of the adjacent subcutaneous fat may be present.

Bone lesions can be seen on T2-weighted sequences secondary to osteolysis, as seen in Gorham-Stout syndrome, also known as disappearing bone disease [12].

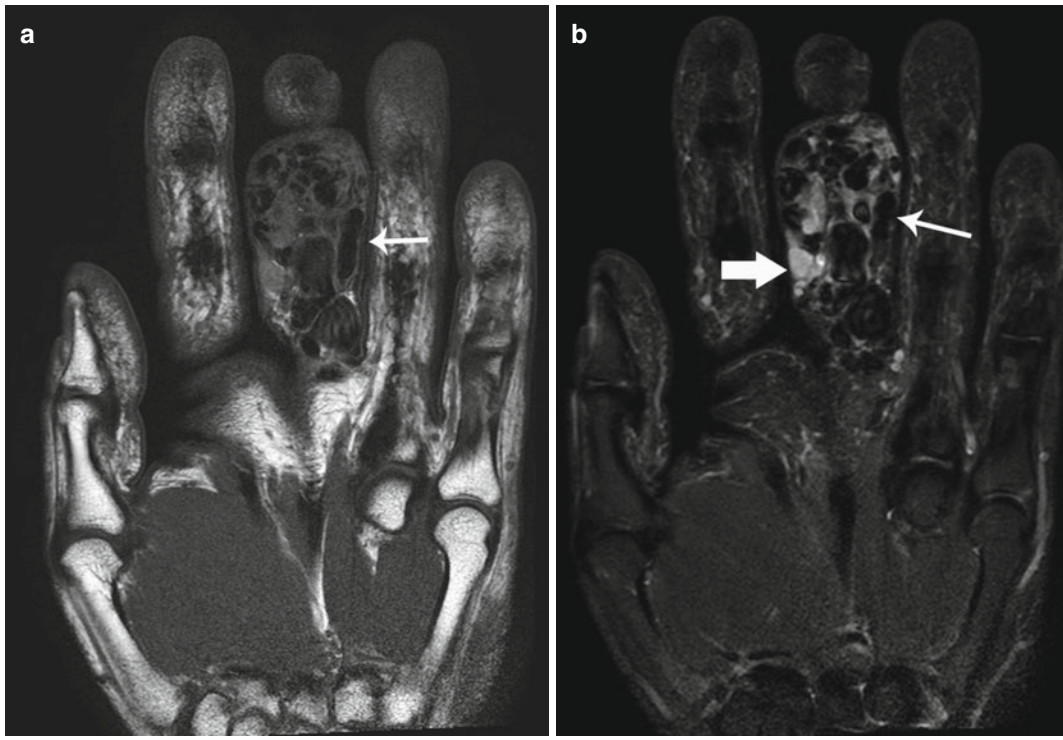

Fig. 27.6 Patient presenting an AVM of the third finger with worsening symptoms of venous congestion. (**a**) T1-weighted spin-echo acquisition showing the high-flow AVM with multiple vascular channels displaying flow void signals (*arrow*). (**b**) T2-weighted short tau inversion recovery (STIR) acquisition showing high-flow vessels with flow void on the arterial and venous side (*small arrow*) and several congestive veins with a low-flow paradoxical enhancement (*large arrow*). (**c**) Time-resolved acquisition (4D track) after gadolinium injection in the arterial phase showing both digital arteries feeding the AVM and the nidus. (**d**) On the venous phase (4D track), the dilated veins and the venous drainage are well demonstrated. (**e**) High-resolution 3D T1-weighted fast-field echo (FFE) with fat suppression in the coronal. It is not possible on these acquisitions to differentiate arterial feeders from draining veins. Small thrombi can be seen on the venous side, probably related to the venous congestion (*arrows*)

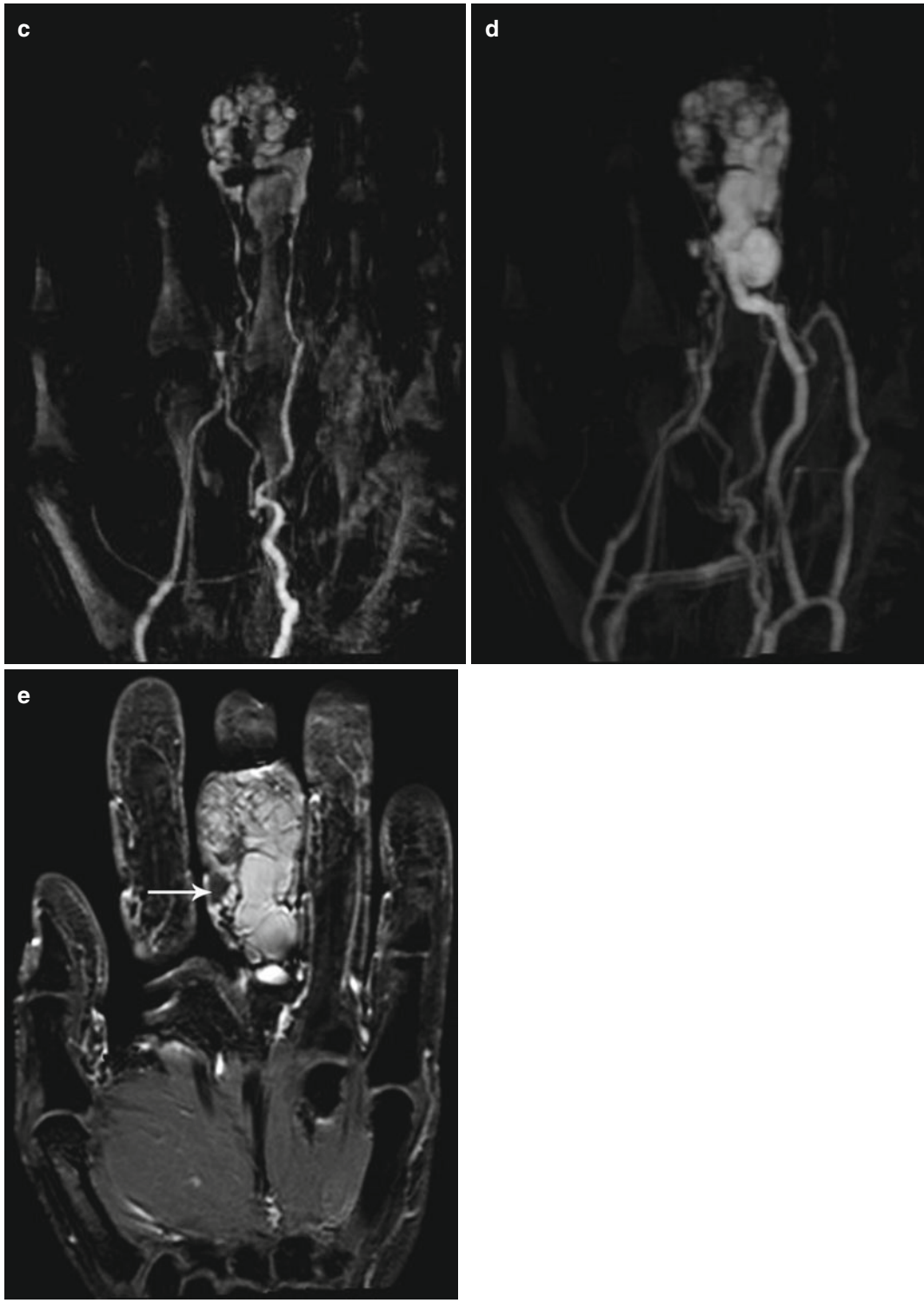

Fig. 27.6 (continued)

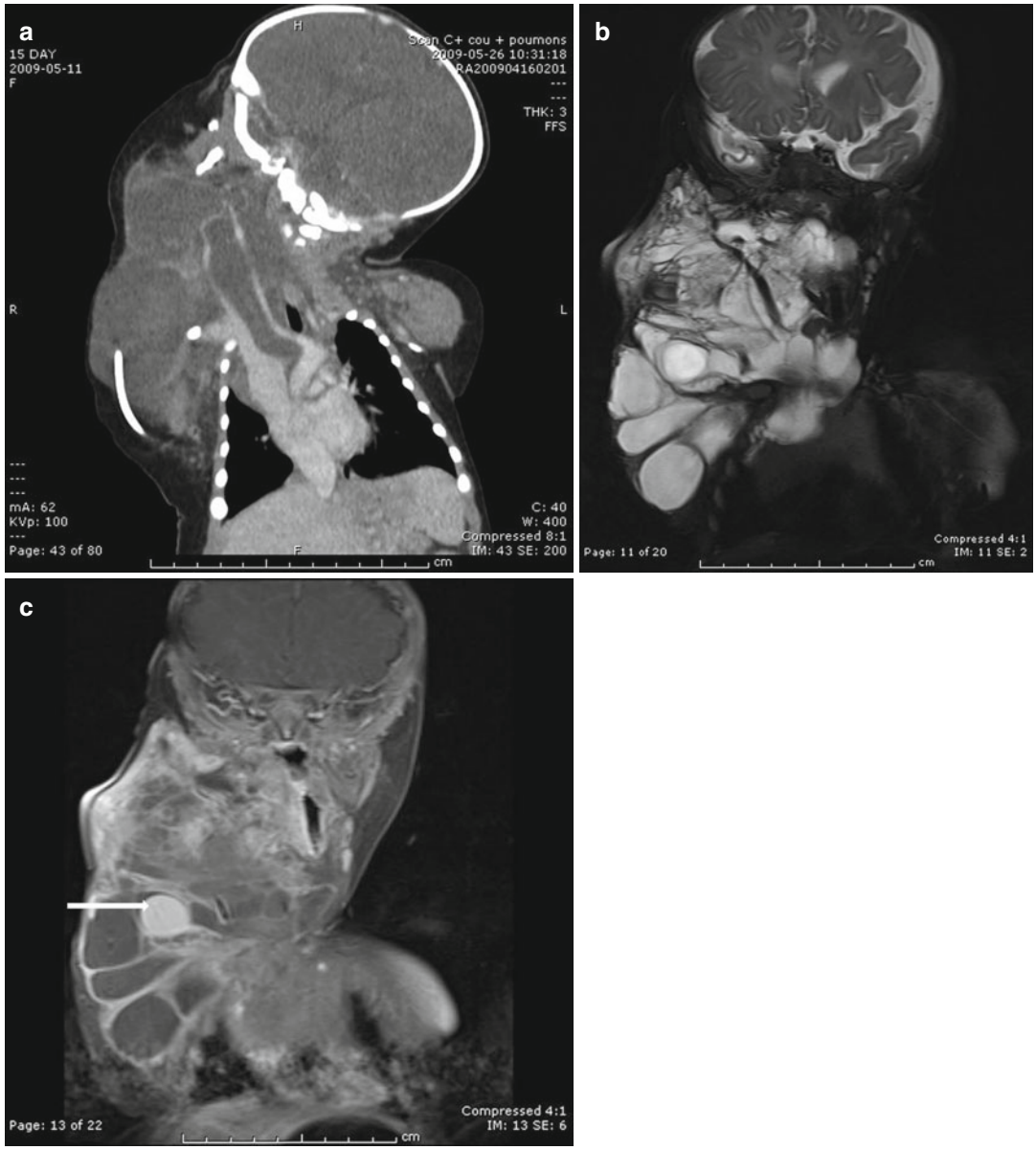

Fig. 27.7 Fifteen-day-old female child with a huge right cervico-mediastinal lesion, confirming a lymphatic malformation diagnosis. (**a**) CT scan shows a hypodense lesion with discrete enhancement of septa and significant displacement of the neck vessels. (**b**) Coronal T2-weighted image demonstrates a hyperintense macrocystic lesion. (**c**) Coronal T1-weighted contrast image shows an enhancement of the septa. The hypersignal in one of the cysts represents hemorrhage (*arrow*)

References

1. Dubois J, Soulez G, Oliva VL, Berthiaume MJ, Lapierre C, Therasse E (2001) Soft-tissue venous malformations in adult patients: imaging and therapeutic issues. Radiographics 21:1519–1531
2. Thawait SK, Puttgen K, Carrino JA, Fayad LM, Mitchell SE, Huisman TAGM, Tekes A (2013) MR imaging characteristics of soft tissue vascular anomalies in children. Eur J Pediatr 172:591–600
3. Caty V, Kauffmann C, Dubois J, Mansour A, Giroux MF, Oliva V, Piché N, Therasse E, Soulez G (2014) Clinical validation of semi-automated software for volumetric and dynamic contrast enhancement analysis of soft tissue venous malformations on magnetic resonance imaging examination. Eur Radiol 24(2): 542–551
4. Dobson MJ, Hartley RW, Ashleigh R, Watson Y, Hawnaur JM (1997) MR angiography and MR imaging of symptomatic vascular malformations. Clin Radiol 52:595–602
5. Ohgiya Y, Hashimoto T, Gokan T et al (2005) Dynamic MRI for distinguishing high-flow from low-flow peripheral vascular malformations. AJR Am J Roentgenol 185:1131–1137
6. Taschner CA, Gieseke J, Le Thuc V et al (2008) Intracranial arteriovenous malformation: time-resolved contrast-enhanced MR angiography with combination of parallel imaging, keyhole acquisition, and k-space sampling techniques at 1.5 T. Radiology 246:871–879
7. Rak KM, Yakes WF, Ray RL et al (1992) MR imaging of symptomatic peripheral vascular malformations. AJR Am J Roentgenol 159:107–112
8. Li W, David V, Kaplan R, Edelman RR (1998) Three-dimensional low dose gadolinium-enhanced peripheral MR venography. J Magn Reson Imaging 8:630–633
9. Reinacher PC, Stracke P, Reinges MH, Hans FJ, Krings T (2007) Contrast-enhanced time-resolved 3-D MRA: applications in neurosurgery and interventional neuroradiology. Neuroradiology 49(Suppl 1):S3–S13
10. Ziyeh S, Strecker R, Berlis A, Weber J, Klisch J, Mader I (2005) Dynamic 3D MR angiography of intra- and extracranial vascular malformations at 3 T: a technical note. AJNR Am J Neuroradiol 26:630–634
11. Dubois J, Alison M (2010) Vascular anomalies: what a radiologist needs to know. Pediatr Radiol 40:895–905
12. Konez O, Vyas PK, Goyal M (2000) Disseminated lymphangiomatosis presenting with massive chylothorax. Pediatr Radiol 30:35–37